Transport Phenomena in Nano and Micro Scales 3 (2015) 14-28

Transport Phenomena in Nano and Micro Scales

journal homepage: http://tpnms.usb.ac.ir/

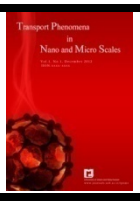

Calculation of Friction Coefficient and Analysis of Fluid Flow in a Stepped Micro-Channel for Wide Range of Knudsen Number Using Lattice Boltzmann (MRT) Method

Y. Bakhshan[1], A.R. Omidvar[2,*]

[1]*Associate professor of Mechanical engineering, Mechanical Engineering Department, University of Hormozgan, Bandar Abbas, I.R.Iran*

[2]*Mechanical Engineering Department, University of Hormozgan, Bandar Abbas, I.R.Iran*

ARTICLE INFO:

Article history:
Received 22 September 2014
Accepted 4 Junuary 2015

Keywords:
Micro-channel
Lattice Boltzmann
Friction Coefficient
Knudsen Number
Gas Flow

Abstract

Micro scale gas flows has attracted significant research interest in the last two decades. In this research, the fluid flow of gases in the stepped micro-channel at a wide range of Knudsen number has been analyzed with using the Lattice Boltzmann (MRT) method. In the model, a modified second-order slip boundary condition and a Bosanquet-type effective viscosity are used to consider the velocity slip at the boundaries and to cover the slip and transition regimes of flow and to gain an accurate simulation of rarefied gases. It includes the slip and transition regimes of flow. The flow specifications such as pressure loss, velocity profile, streamline and friction coefficient at different conditions have been presented. The results show good agreement with available experimental data. The calculation shows that the friction coefficient decreases with increasing the Knudsen number and stepping the micro-channel has an inverse effect on the friction coefficient. Furthermore, a new correlation is suggested for calculation of the friction coefficient in the stepped micro-channel as below;

$$C_f Re = 3.113 + \frac{2.915}{1 + 2\,Kn} + 0.641\,exp\left(\frac{3.203}{1 + 2\,Kn}\right)$$

1. Introduction

Fluid Flow in macro devices is different from micro devices, because the Navier-Stokes equations based on the continuum flow model is not valid when the characteristics length of the flow domain decreasing. When the mean free path of the molecules is comparable to the characteristic length, this phenomenon is called rarefaction effect [1] and the flow rate in micro channels cannot be predicted with theories based on the continuum flow model. The most important dimensionless parameter in micro-scale gas flows is the Knudsen number, The Knudsen number is defined as the ratio of the molecular mean

*Corresponding author
Email address: alireza9359300@yahoo.com

Nomenclature

B	molecular slip coefficient
C	lattice speed
C_i	discrete velocity vectors
C_s	Sound of speed in lattice scale
C_f	Skin friction coefficient
f	particle distribution function
H	height of the channel (m)
j	Speed in momentums space
Kn	Knudsen number (Kn=λ/H)
m	distribution function in MRT
M	transform matrix
n	wall normal coordinate
p	Pressure ($N.m^{-2}$)
r	Bounce back fraction parameter
R	gas constant
Re	Reynolds number (Re=ρvH/μ)
S	relaxation time diagonal matrix
t	Time (s)
T	Temperature (k)
u	Velocity ($m.s^{-1}$)
w_i	weight factors

Greek Symbols

ρ	Density ($kg.m^{-3}$)
λ	Molecular mean free path (m)
ξ	Sound speed
Ω	collision operator
∇	gradient
τ	non-dimensional relaxation time
τs	relaxation time (Based on viscosity)
τq	relaxation time (Based on slip boundary)
υ	kinematic viscosity ($m^2.s^{-1}$)
μ	dynamic viscosity ($N.s.m^{-2}$)
π	Pi number (3.14159)
σ	TMAC coefficient

Subscripts/Superscripts

eq	equilibrium
i	discrete Lattice directions
eff	effective
out	outlet
in	inlet
ρ	density (relaxation time)
e	energy (relaxation time)
~	Pre collision
w	wall

free path (λ) to the characteristic length of system and increasing of it, causes the changing of a flow regime from the continuum to slip and transition mode.

Thus, the Knudsen number is a measure of rarefaction of gases encountered in flows through very small size channels, and also is a measure of the degree of validity of the continuum mode. The existence of slip velocity at the wall was first predicted by Maxwell [2]. Because of the slip at the walls, the flow rate in micro devices is higher than predicted from no-slip boundary conditions. Based on the Knudsen number, the flow regime can be categorized into four groups: continuum flow (Kn < 0.01), slip flow (0.01 < Kn < 0.1), transition flow (0.1 < Kn < 10), and free molecular flow (Kn > 10) [3]. Micro devices work with a range of Knudsen numbers in different part of the devices, this fact makes it even more difficult to develop a generalized CFD model. By reducing the dimension of a channel, heat transfer coefficient increases significantly. Therefore, micro scale gas flows have attracted the interests of the researchers and received considerable attention in the past decades. Various flow phenomenon were observed in micro-scales that makes it different from macro scales, such as: slip flow, temperature jump, rarefaction, compressibility, intermolecular forces, and viscous dissipation. For the transition and free molecular regimes, it is accepted that the continuity assumption and consequently, the validity of classical description based on the Navier-Stokes equations (NSE) is questionable, because as the size is reduced the flow behavior depends strongly on the geometry dimension, and rarefaction effects dominate the flow characteristic [4]. Molecular based method such as molecular dynamics (MD) and direct simulation Monte Carlo (DSMC) may be used to simulate rarefied gas flows in transition flow regimes. However, simulations on the molecular level are still too expensive for the most practical application, so a midway approach for the flow simulation which can be considered as a particle based method and at the same time is independent of the actual number of molecule is needed. An approach that has some benefits to other's methods, is the Lattice Boltzmann method (LBM); because the LBM is a Mesoscopic method and due to its kinetic origin, it requires less computational cost, and the structure of the LBE is very simple. The important reason that makes the LBM more popular method than other methods, it can be easily implemented on parallel computers [5].

Therefore, the LBM can be used to simulate fluid flows in all regimes upon appropriate adjustments [6]. The investigation of micro scale gas flows have been made by the different methods, such as: experimental work, analytical, and numerical simulations. Arkilic et al. [7], investigated on straight micro channels and its work was in good agreement with experimental data of pong et al. [8]. Beskok et al. [9] performed numerical simulations to investigate the effects of compressibility and rarefaction with the first-order slip boundary condition in micro channels flows. Investigations of Colin et al. [10] show, that the accuracy of the first-order slip boundary condition is not valid when the Knudsen is larger than 0.05. In recent efforts, the main focus was on developing LB models for rarefied gaseous flow in slip flow regimes [11-17], but only a few papers have been focused on LBM in transition flow regimes[18-23].Two approaches are proposed to increase the accuracy of the LBM, the first approach is to use the higher-order LBM via increasing the number of discrete velocity [18-19, 24-28]. Kim et al.[29,30] Zhang et al.[31,32] recently found that the accuracy of higher-order LB models for rarefied gas flows cannot predict the mass flow rate properly.

Succi [33] additionally found that the higher-order LBM with a large number of discrete velocities are not numerically stable. Another approach is to make use of an effective viscosity [12-19] for high Kn number. Recently, flows through more complicated geometries have been studied. Oliveira et al.[34], numerically and experimentally studied constricted micro channels and Liou et al. [35] numerically studied micro channel with expansion and contraction for a wide range of Kn number in slip flow regimes. The above summary shows that, the experimental measurements, and numerical simulations of gas flows in straight micro channels have already been extensively studied in slip flow regimes but only a few papers can be mentioned in transition flow regimes. However, few studies have been given to complex micro channel flows especially under a wide range of Knudsen number in slip and transition flow regimes.In this study, the fluid flow of gases in a stepped micro channel has been studied for a wide range of Knudsen numbers that shows the regimes of flows with using Lattice Boltzmann method. The friction coefficient is an important parameter which must be analyzed to estimate wall shear rate to balancing between heat removing and shear stress at the wall if we use the micro-channel for increasing of heat transfer coefficient or stepping the micro-channel**.** In this study, the friction coefficient in the micro-channel is calculated and a new correlation is suggested for it. The two cases of constant Knudsen number and variable Knudsen number have been conducted for calculation of flow specifications and friction coefficient.

2. Governing Equations and Numerical Procedure

2.1. Boltzmann equations

The continuum Boltzmann equation is a fundamental equation for rarefied gases flows in the kinetic theory. It considers the collective behavior of molecules in a system. For system without an external force, the Boltzmann equation can be written as;

$$\frac{\partial f}{\partial t} + \vec{\xi}.\nabla f = \Omega(f, f') \tag{1}$$

where $f(\vec{x},\vec{\xi},t)$ is the single particle distribution function (the probability of finding particle within a certain range of velocity $\vec{\xi}$ at a certain range of location $\vec{x}$ at a given time t) and Ω is the collision operator. The collision operator Ω is a nonlinear integral term, in which f and $f'$are pre and post collision distribution functions. The simplified model for collision operator is:

$$\Omega = -\frac{1}{\lambda}(f - f^{eq}) \tag{2}$$

where λ is called relaxation time, and f^{eq} is the equilibrium distribution function approximated as Maxwellian form as blow;

$$f^{eq} = \frac{\rho}{(2\pi RT)^{\frac{3}{2}}} \exp\left(-\frac{(\vec{\varepsilon} - \vec{u})^2}{2RT}\right) \tag{3}$$

where R is the gas constant and ρ, $\vec{u}$ and T are density, velocity and temperature, respectively. This model known as the (BGK) model.

By using BGK approximation Equation 1 can be re-written as below;

$$\frac{\partial f}{\partial t} + \vec{\xi}.\nabla f = -\frac{1}{\lambda}(f - f^{eq}) \tag{4}$$

2.2. SRT and MRT schemes of Lattice Boltzmann

In lattice Boltzmann method, assumed Equation 4 is valid along specific directions, so it can be written as;

$$\frac{\partial f_i}{\partial t} + \vec{\xi}_i \cdot \nabla f_i = -\frac{1}{\lambda}(f_i - f_i^{eq}) \tag{5}$$

By discretization of Equation 5, in space (x) and time (t). The lattice Boltzmann equation without external force is given by;

$$f_i(\vec{x} + \vec{c}_i dt, t + dt) - f_i(\vec{x}, t) = -\frac{1}{\tau}\left(f_i(\vec{x}, t) - f_i^{eq}(\vec{x}, t)\right) \tag{6}$$

where $\tau = \frac{\lambda}{\Delta t}$, is the non-dimensional relaxation time. This model known as the lattice Boltzmann single relaxation time (SRT). Another approximation is the model with multiple relaxation time (MRT) collision operators. MRT scheme offers a higher stability and accuracy than SRT scheme. Collision operator in MRT method is defined as bellows;

$$\Omega_i = -(M^{-1}SM)_{ij}\left[f_j - f_j^{eq}\right] \tag{7}$$

where S is a diagonal matrix $S = diag(\tau_0, \tau_1, \dots, \tau_i)^{-1}$ and M is the transform matrix projecting the distribution function to the moment space and is given by;

$$m = Mf \tag{8}$$

In this work, we used the two dimensional nine velocity (D2Q9) model and is shown schematically in the figure 1.
This model is very suitable for solving of fluid flow problems in two-dimensional flow systems. in D2Q9 model the velocity set is given by:

$$\vec{c}_i = \begin{cases} (0,0), & i = 0 \\ \left(\cos\left(\frac{i-1}{2}\pi\right), \sin\left(\frac{i-1}{2}\pi\right)\right)c, & i = 1, \dots, 4 \\ \sqrt{2}\left(\cos\left(\frac{2i-9}{4}\pi\right), \sin\left(\frac{2i-9}{4}\pi\right)\right)c, & i = 5, \dots, 8 \end{cases} \tag{9}$$

The equilibrium distribution function followed by discretization of the D2Q9 lattice nodes is obtained as below

$$f_i^{eq} = \rho w_i\left[1 + \frac{\vec{c}_i . u}{c_s^2} + \frac{(\vec{c}_i . u)^2}{4c_s^2} - \frac{u^2}{2c_s^2}\right] \tag{10}$$

where $c_s = \sqrt{RT} = \frac{c}{\sqrt{3}}$ is the sound speed, R is the gas constant, T is the temperature, and w_i are weight factors and is given by;

$$\vec{w}_i = \begin{cases} \frac{4}{9}, & i = 0 \\ \frac{1}{9}, & i = 1, \dots, 4 \\ \frac{1}{36}, & i = 5, \dots, 8 \end{cases} \tag{11}$$

We used the relaxation matrix S and transform matrix M given by Lallemand et al. [26];

$$S = diag(\tau_\rho, \tau_e, \tau_\varepsilon, \tau_j, \tau_q, \tau_j, \tau_q, \tau_s, \tau_s)^{-1} \tag{12}$$

$$M = \begin{pmatrix} 1 & 1 & 1 & 1 & 1 & 1 & 1 & 1 & 1 \\ -4 & -1 & -1 & -1 & -1 & 2 & 2 & 2 & 2 \\ 4 & -2 & -2 & -2 & -2 & 1 & 1 & 1 & 1 \\ 0 & 1 & 0 & -1 & 0 & 1 & -1 & -1 & 1 \\ 0 & -2 & 0 & 2 & 0 & 1 & -1 & -1 & 1 \\ 0 & 0 & 1 & 0 & -1 & 1 & 1 & -1 & -1 \\ 0 & 0 & -2 & 0 & 2 & 1 & 1 & -1 & -1 \\ 0 & 1 & -1 & 1 & -1 & 0 & 0 & 0 & 0 \\ 0 & 0 & 0 & 0 & 0 & 1 & -1 & 1 & -1 \end{pmatrix} \tag{13}$$

Based on D2Q9 model, we can define distribution function and equilibrium distribution function in MRT model as follows;

$$m = Mf \tag{14}$$

$$m^{eq} = Mf^{eq} = \begin{pmatrix} \rho, & e^{eq}, & \varepsilon^{eq}, & j_x, & q_x^{eq}, & j_y, & q_y^{eq}, \\ & & p_{xx}^{eq}, & & p_{xy}^{eq} & & \end{pmatrix}^T = Mf^{eq} = \rho\begin{pmatrix} 1, -2 + 3|u|^2, 1 - 3|u|^2, u, -v, \\ u, -v, u^2 - v^2, uv \end{pmatrix}^T \tag{15}$$

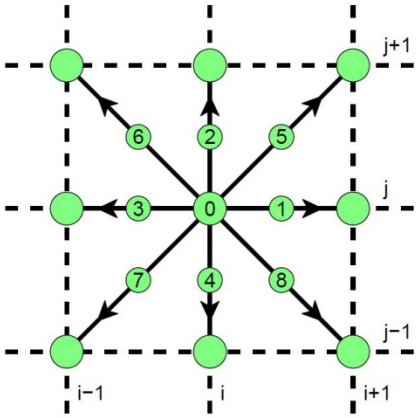

Fig. 1. Discrete velocity vectors for D2Q9 lattices

The macroscopic parameters such as density ρ, velocity u, and pressure p are calculated in terms of the distribution function as follows;

$$\rho = \sum_i f_i \tag{16}$$

$$\rho\vec{u} = \sum_i \vec{c}_i f_i \tag{17}$$

$$p = \rho c_s^2 \tag{18}$$

2.3. LBM for high Knudsen number

According to the Chapman–Enskog expansion, kinematic viscosity can be written as:

$$\upsilon = c_s^2 \delta t(\tau_s - 0.5) \tag{19}$$

Based on [36], relaxation time (τ_s) is a free parameter, but in a micro-channel simulation it must be defined correctly to obtain accurate slip velocity at the wall.

The first step in simulation of micro scale gas flows is defining the relation between the relaxation time and the Knudsen number. Based on the inverse power law (IPL) model, the mean free path (λ) of gas is given by[37]:

$$\lambda = \frac{\mu}{p}\sqrt{\frac{\pi RT}{2}} \tag{20}$$

Finally, from Eqs. (19) and (20), the relaxation time (τ_s) can be expressed as a function of the Knudsen number (Kn) and height of the channel (H) as follows:

$$\tau_s = 0.5 + \sqrt{\frac{6}{\pi}}\mathrm{KnH} \tag{21}$$

In the limit of the Kn<<1, the molecule-wall collisions can be neglected compared with the intermolecular collision, but for gas flows at high Knudsen number, due to the effect of the Knudsen layer near the solid wall, collision between gas molecule and the walls are the dominant phenomenon, and the inter molecular collisions are reduced with the increase of the rarefaction effect. In the free molecular flow limit Kn>>1 only the collision of the gas molecule with the wall should be considered.[9], So Viscosity and the mean free path given by Eq. (20) are only valid in unbounded gas flow region and must be corrected. In the literature, some formulation has been proposed from different point of view [27]. We used the effective viscosity proposed by Beskok et al. [9]here and is below;

$$\mu_{eff} = \frac{1}{1 + f(Kn)}\mu \ , f(Kn) = aKn \tag{22}$$

Several models have been proposed for calculation of f(Kn) which are based on numerical and analytical data.

For instance, Beskok et al.[9] used a=2.2 with their calculation and Michalis et al. [28] investigated the rarefaction effect on gas viscosity using the DSMC method, and suggested a value near to 2 for a.

According to the equation 21 and effective viscosity, relaxation time should be defined as;

$$\tau_s = 0.5 + \sqrt{\frac{6}{\pi}}\frac{\mathrm{KnH}}{(1 + f(Kn))} \tag{23}$$

At low Knudsen numbers, due to its definition, the mean free path is a key parameter, so with decreasing the Kn, its value will decrease and thus the compressibility of flow will increase.

Mean free path is inversely proportional to the pressure, so variation of the local Knudsen number along the channel can be expressed as

$$Kn(x) = \frac{Kn_{out}P_{out}}{P(x)} \tag{24}$$

where the quantities with the (out) subscript represents the values at the outlet of channel and p(x) and Kn(x) is the local pressure and Knudsen along the centerline of channel.

2.4. Boundary Conditions for LBM

To simulate various flow regimes such as slip and transition flow in the micro channels, suitable boundary conditions must be applied for isothermal rarefied gas, when an effective viscosity is used. We used the second-order slip boundary condition as follows;

$$u_s = B_1\sigma_V\lambda_e\frac{\partial u}{\partial n}|_w - B_2\lambda_e^2\frac{\partial^2 u}{\partial n^2}|_w \quad (25)$$

where λ_e is the mean effective free path, n is the wall normal coordinate pointing into the fluid, and $\sigma_V = \frac{2-\sigma}{\sigma}$, in which σ is the tangential momentum accommodation coefficient (TMAC). We denotes the quantity at the wall, and $B_1 = (1 - 0.1817\sigma)$. B_2 Plays an important role for the second-order order slip boundary condition in simulating rarefied gas flow with relatively large Knudsen number and $B_2 = 0.8$ is the best fit to the solution of linearized Boltzmann equation.

Second-order slip boundary conditions at the lower wall are given by;

$$f_2 = \widetilde{f_4},\quad f_5 = r\widetilde{f_7} + (1-r)\widetilde{f_8}$$
$$f_6 = r\widetilde{f_8} + (1-r)\widetilde{f_7} \quad (26)$$

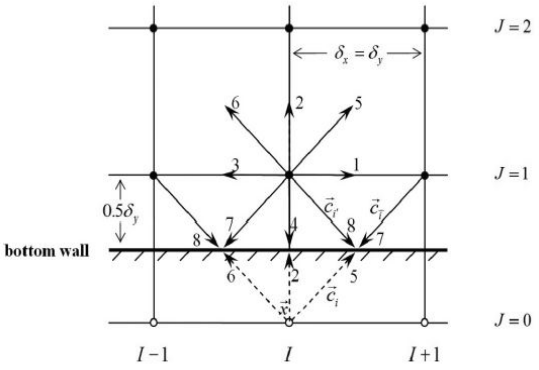

Fig. 2. Schematic diagram for boundary condition at the bottom wall

where $\widetilde{f_r}$ are post collision distribution function at j=1 (Figure 2), (The wall is located at j=0.5), to match the second-order slip boundary condition, the bounce back fraction parameter r and relaxation time τ_q are chosen as;

$$r = \frac{1}{1 + B_1\sigma_V\sqrt{\frac{\pi}{6}}}, \quad \tau_q = \frac{1}{2} + \frac{3 + 4\pi\tilde{\tau}_s^2 B_2}{16\,\tilde{\tau}_s^2} \quad (27)$$

where $\tilde{\tau}_s = \tau_s - 0.5$.

2.5 Boundary Conditions at inlet and outlet

In this work, pressure (density) boundary condition is used at inlet and outlet of the flow domain. The unknown distribution functions at the inlet and outlet have been evaluated after the streaming step. With supposing the specified density at the inlet of flow boundary (For example in the Figure 3) along the y-direction, and the specified u_y (e.q., $u_y = 0$ at the inlet in a channel flow), after streaming, f_2, f_3, f_4, f_6, f_7 are obtained and for determining the u_x and f_1, f_5, f_8 the following equations are used:

$$f_1 + f_5 + f_8 = \rho_{in} - (f_0 + f_2 + f_3 + f_4 + f_6 + f_7) \quad (28)$$

$$f_1 + f_5 + f_8 = \rho_{in}u_x + (f_3 + f_6 + f_7) \quad (29)$$

$$f_5 - f_8 = -f_2 + f_4 - f_6 + f_7 \quad (30)$$

So, with consistency of Equations 28 and 29 gives;

$$u_x = 1 - (f_0 + f_2 + f_4 + 2(f_3 + f_6 + f_7)/\rho_{in} \quad (31)$$

Also we used the bounce-back rule for the non-equilibrium part of the particle distribution to find $f_1 - f_1^{eq} = f_3 - f_3^{eq}$ which are normal to the inlet. With f_1 value, f_5 and f_8 are obtained by the remaining equations as blow;

$$f_1 = f_3 + \frac{2}{3}\rho_{in}u_x \quad (32)$$

$$f_5 = f_7 - \frac{1}{2}(f_2 - f_4) + \frac{1}{6}\rho_{in}u_x \quad (33)$$

$$f_8 = f_6 + \frac{1}{2}(f_2 - f_4) + \frac{1}{6}\rho_{in}u_x \quad (34)$$

The corner nodes at the inlet are crucial for the simulations.

The constant pressure boundary conditions are not applicable here, because the inlet pressure condition must be consistent with the flow field inside the channel. After streaming, f_3, f_4, f_7 are obtained and with specified density and $u_y = 0$ we determine f_1, f_2, f_5, f_6, f_8, as blow;

$$f_1 = f_3 + \frac{2}{3}\rho_{in} u_x \quad (35)$$

$$f_2 = f_4 \quad (36)$$

$$f_5 = r f_7 + (1-r) f_8 \quad (37)$$

$$f_6 = r f_8 + (1-r) f_7 \quad (38)$$

$$f_8 = f_7 + \frac{1}{6}\rho_{in} u_x (1-r) \quad (39)$$

So, with consistency of Equations (28-39) gives;

$$u_x = \frac{\left[1 - \frac{[f_0 + f_2 + f_4 + 2(f_3 + f_6 + f_7)]}{\rho_{in}}\right]}{\left[1 + \frac{r}{3(1-r)}\right]} \quad (40)$$

A similar procedure has been applied to the top inlet node and outlet nodes.

2.6. Grid Generation

For grid generation, we used structural scheme with equal dimension in the both x and y directions. For the micro-channel without step, the total 2100(N_x=2100) and 21(N_y=21) lattice nodes have been considered in the x and y directions respectively.

Figure 3 shows, the considered grid schematically. Figure 4 shows, the generated and used grids at the boundary of flow field.

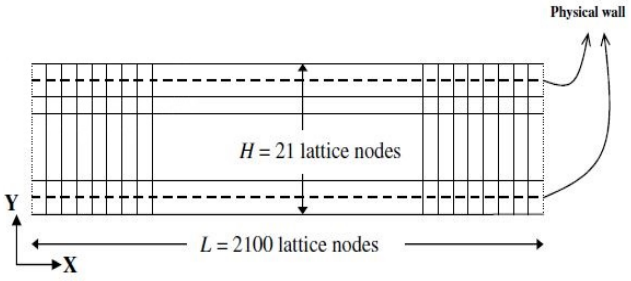

Fig.3. The used schematic geometry for grid generation

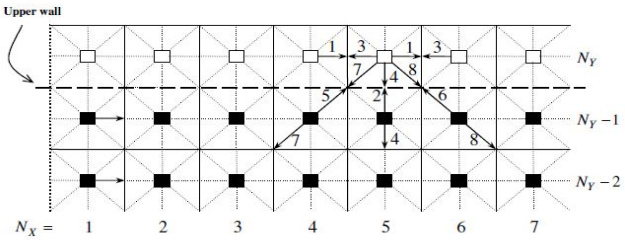

Fig.4. The used grids at the boundary of geometry

Figure 5 shows, the used geometry for stepped micro-channel, so with considering the following dimensions, the generated grids at the steps are shown in the figure 6.

L_u=L_d=2000, W_u=40, W_c=20, L_c=40, L_s=20

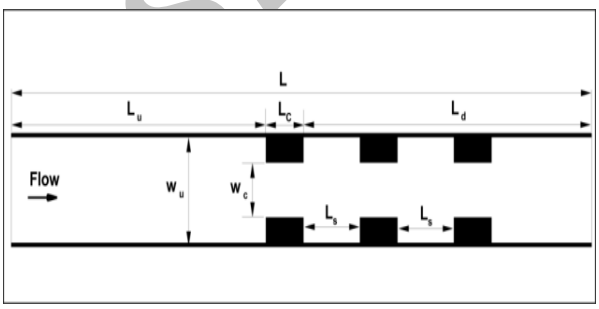

Fig. 5. The used geometry with step

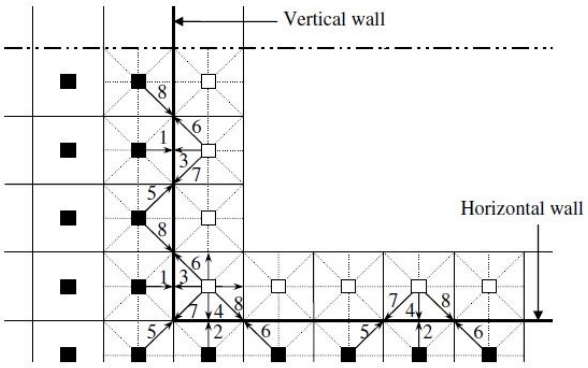

Fig. 6. The generated grids at the steps

3. Results and discussion

The used geometry in our simulation is shown schematically in figure 7. The micro-channel stepped in three locations with variable dimensions and the parametric study can be conducted. The prepared

computer code has ability to consider the wide range of Knudsen number and it can calculate the flow specifications in different regimes, so we compared the extracted results with the other semi-empirical or theoretical available results.

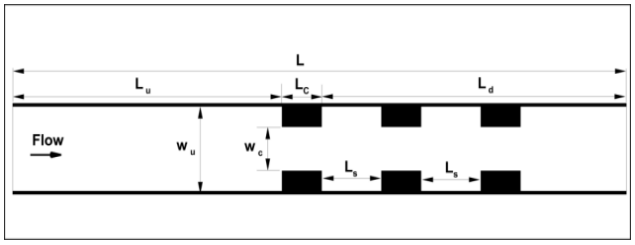

Fig. 7. The used schematic geometry

Figure 8, Shows the flow rate of fluid in the micro-channel versus Knudsen number. The calculation has been donned with using the lattice Boltzmann method and compared with kinetic theory and the work of Ohwada et al[25]. This comparison shows, the LBM has good accuracy for prediction of fluid flow specifications at low and medium Knudsen numbers and its accuracy has much deviation at high Knudsen numbers, but the LBM accuracy increased with increasing Knudsen numbers.

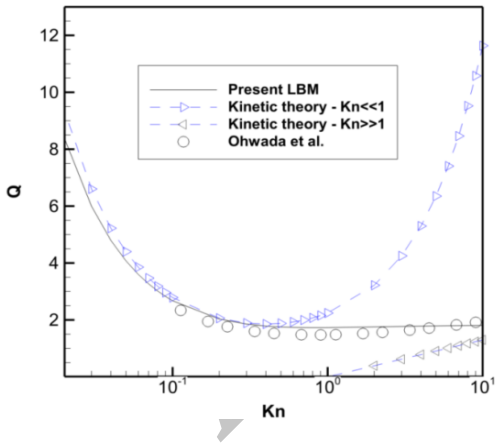

Fig. 8. Flow rate variation versus Knudsen number

Figure 9, Shows the non-dimensional pressure loss throughout the micro-channel and compares the calculation results with experimental data of Arkilic et al.[7]. For consistence, we applied one step in the micro-channel. The pressure loss at the step is clear and the results have good agreement with experimental data. Figures (10-13) show, the non-dimensional velocity profiles at different Knudsen numbers and compare the calculated results with results of Ohwada et al. [25]. and the result have good agreement with the work of Ohwada et al [25]. It is notified that this comparison is donned without stepping the micro-channel.

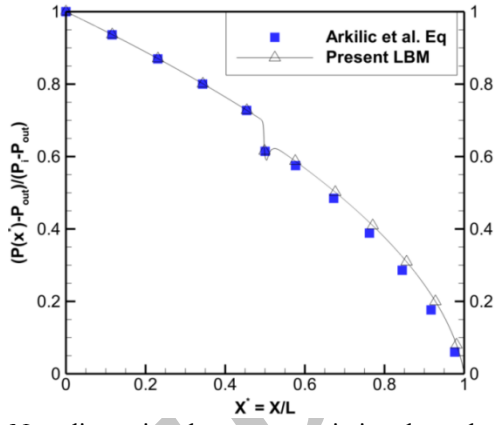

Fig. 9. Non-dimensional pressure variation throughout the micro-channel

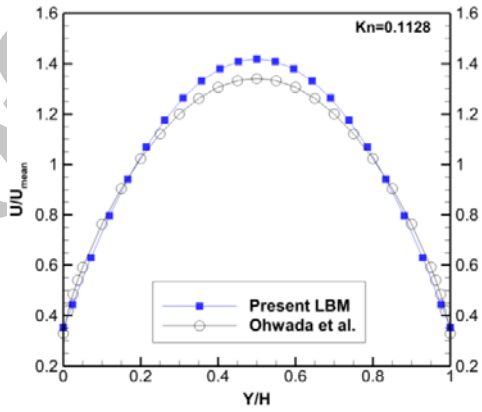

Fig. 10. Velocity profile at outlet cross section at Knudsen number=0.1128

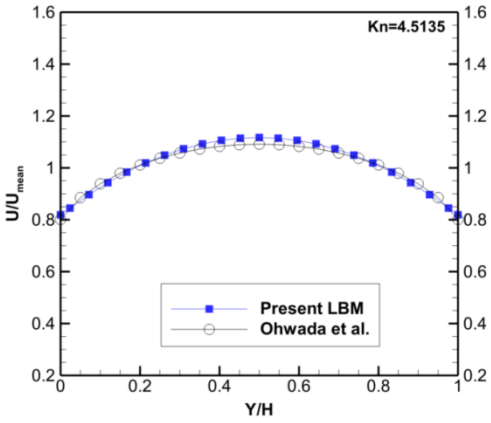

Fig. 11. Velocity profile at outlet cross section at Knudsen number=4.5135

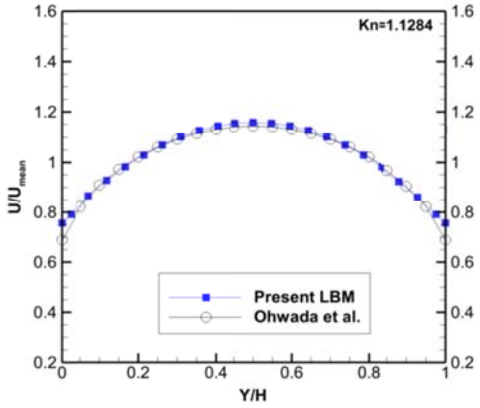

Fig. 12. Velocity profile at outlet cross section at Knudsen number=1.1284

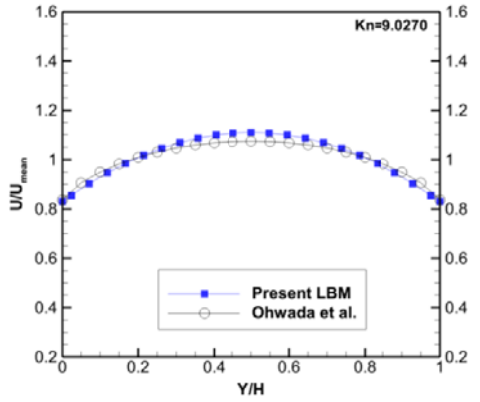

Fig. 13. Velocity profile at outlet cross section at Knudsen number=9.0270

Figures (14-18), show the streamlines of fluid flow in the micro-channel at different Knudsen numbers for two pressure ratio. With increasing the Knudsen number, the size of formed vortexes after steps will decrease but they will stretch in longitudinal and with increasing the pressure ratio, the size of vortexes will increase in general and this causes the larger pressure loss in higher pressure ratio. By increasing the pressure ratio, the swirl ratio at the center of wakes will increase and this results the back flow after the steps. Increasing the Knudsen number causes, the increasing of slip velocity at the walls and it is observed the curvature of the velocity at the cross section of channel becomes flatter (Figure19). At the low Knudsen numbers the compressibility of fluid is high and the fluid flow is continuum approximately and this causes the high kinetic energy at the center of channel. Figures (20-26), show the velocity profile at four locations (near to step, on the step, after step and between two steps) of micro-channel. With increasing the pressure ratio, and lowering Knudsen number the fluid flow behavior tends to be continuum and backflow after steps is clear Figure 21.

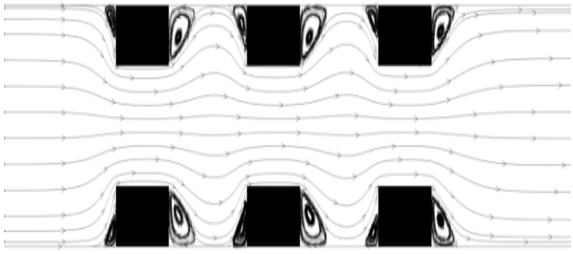

Fig. 14. Streamlines in the micro-channel at Pi/Po=2, Knudsen number=0.01

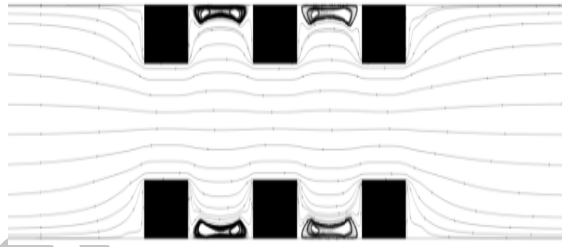

Fig. 15. Streamlines in the micro-channel at Pi/Po=2, Knudsen number=2

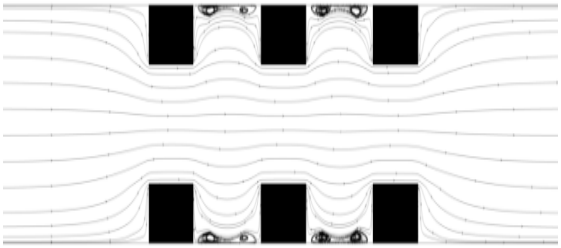

Fig. 16. Streamlines in the micro-channel at Pi/Po=2, Knudsen number=0.5

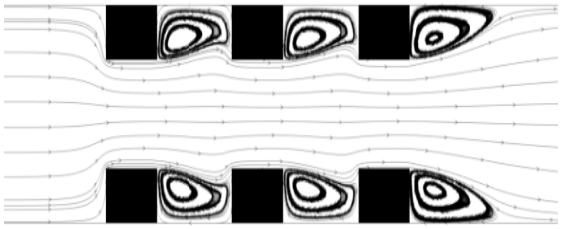

Fig. 17. Streamlines in the micro-channel at Pi/Po=5, Knudsen number=0.01

Figures (27-30), show the centerline velocity throughout of micro-channel with and without steps at different pressure ratio. For the case of low pressure ratio, Pi/Po=2, flow decelerate and pressure decreases

(Figure 31) suddenly at the steps to maintain the mass conservation.

From figures (27-30), it is founded, the centerline velocity increases gradually due to pressure loss in the micro-channel and a sudden increasing of velocity at steps location is observed. The slope of velocity at low Knudsen number (0.01) is greater than high Knudsen numbers and the importance of steps is highlight at low Knudsen numbers.

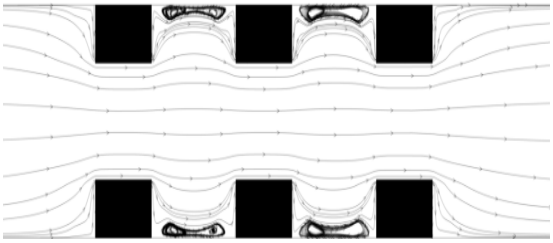

Fig. 18. Streamlines in the micro-channel at Pi/Po=5, Knudsen number=2

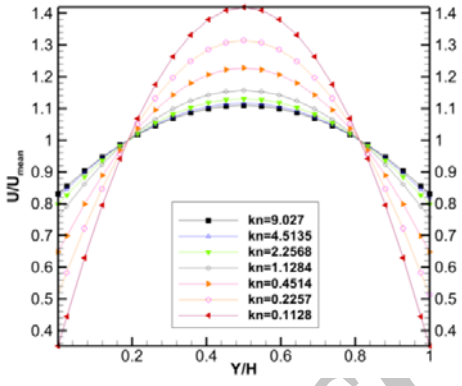

Fig. 19. Velocity profiles at different Knudsen numbers

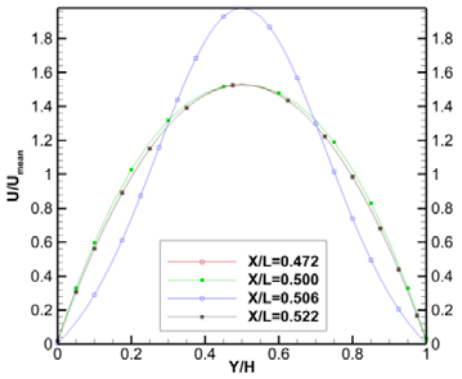

Fig. 20. Velocity profile at different cross sections at Pi/Po=2, Outlet Knudsen number=0.01

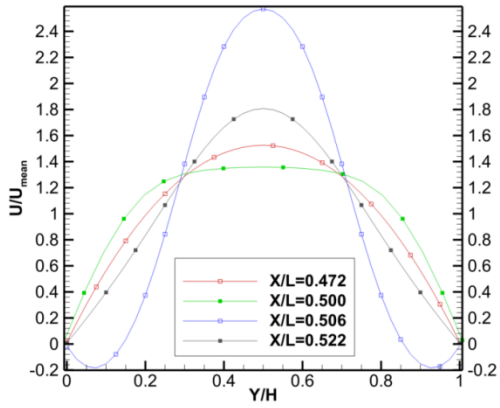

Fig. 21. Velocity profile at different cross sections at Pi/Po=5, Outlet Knudsen number=0.01

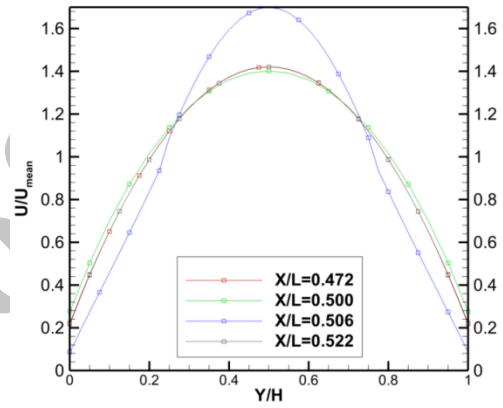

Fig. 22. Velocity profile at different cross sections at Pi/Po=2, Outlet Knudsen number=0.1

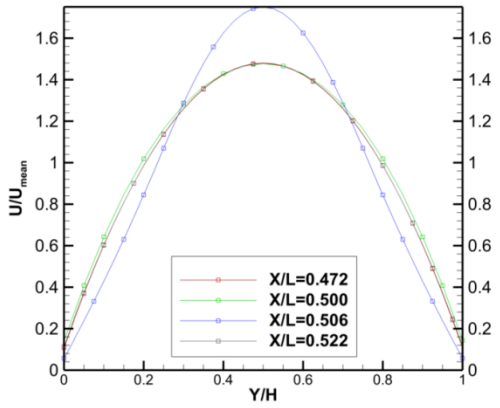

Fig. 23. Velocity profile at different cross sections at Pi/Po=5, Outlet Knudsen number=0.1

Figures 31and 32, show the pressure losses throughout the micro-channel at different outlet Knudsen numbers and for two different pressure ratio. The pressure losses at steps locations is clear from these

figures and has same tracing for all Knudsen numbers but with increasing the pressure ratio, the pressure loss takes larger values.

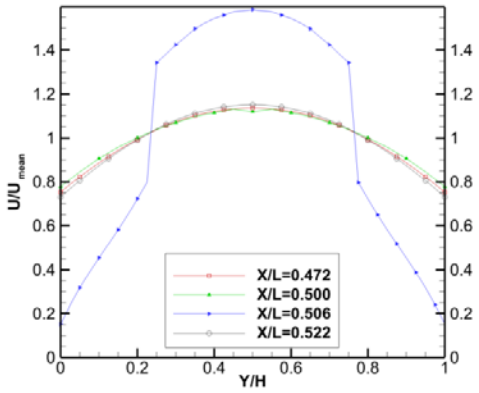

Fig. 24. Velocity profile at different cross sections at Pi/Po=2, Outlet Knudsen number=2

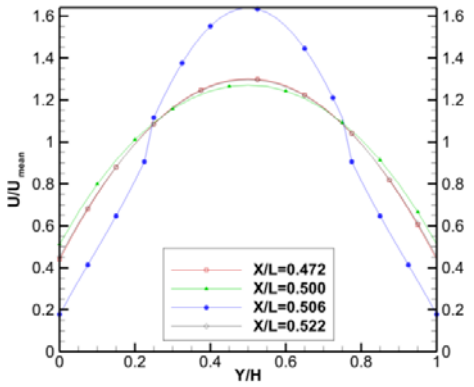

Fig. 25. Velocity profile at different cross sections at Pi/Po=5, Outlet Knudsen number=0.5

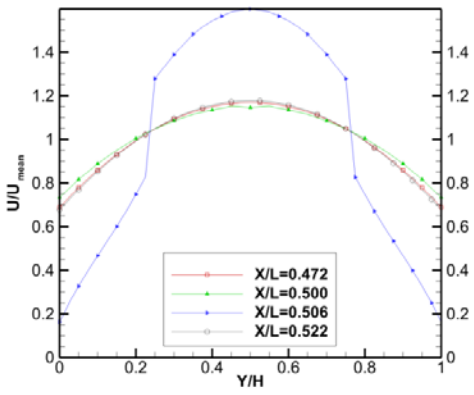

Fig. 26. Velocity profile at different cross sections at Pi/Po=5, Outlet Knudsen number=2

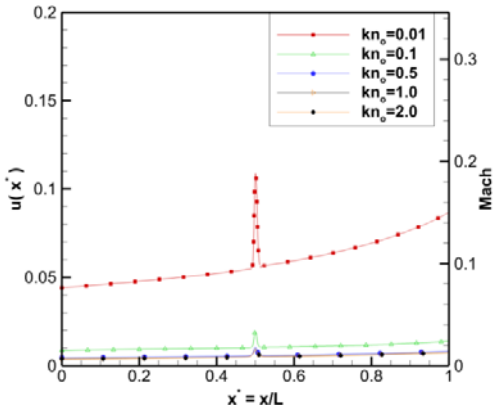

Fig. 27. Centerline velocity profile at different outlet Knudsen numbers and Pi/Po=2, 1 step

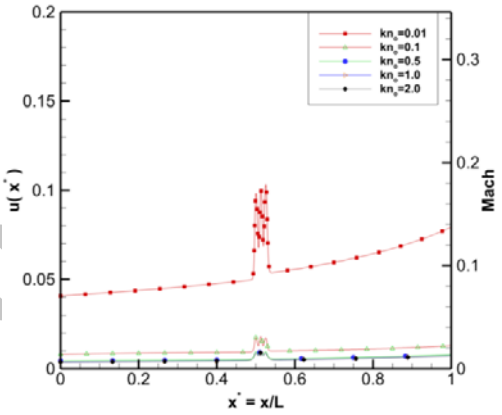

Fig. 28. Centerline velocity profile at different outlet Knudsen numbers and Pi/Po=2, 3 step

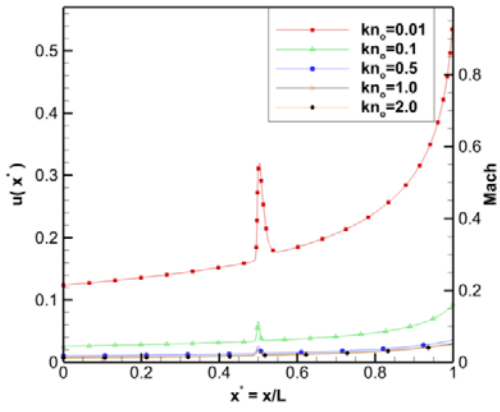

Fig. 29. Centerline velocity profile at different outlet Knudsen numbers and Pi/Po=5, 1 step

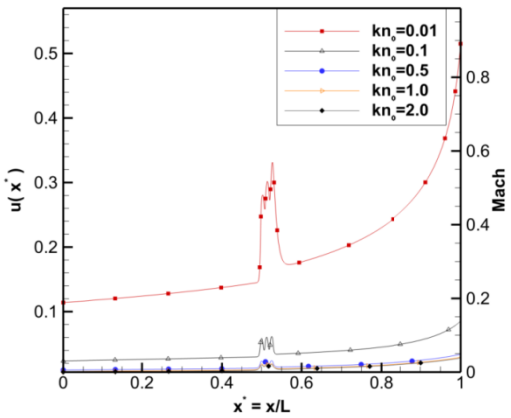

Fig. 30. Centerline velocity profile at different outlet Knudsen numbers and Pi/Po=5, 3 step

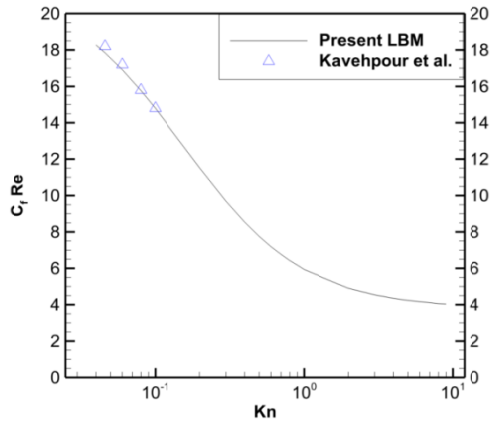

Fig. 33. Variation of friction coefficient versus Knudsen number

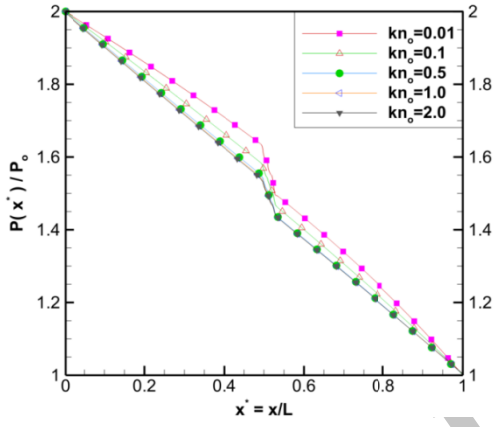

Fig. 31. Centerline pressure profile at different outlet Knudsen numbers and Pi/Po=2, Pressure Loss, 3 step

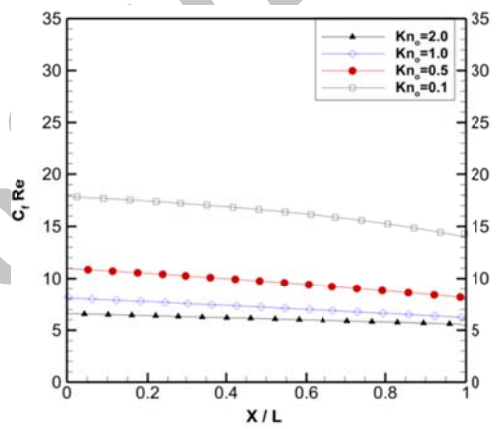

Fig. 34. Variation of friction coefficient throughout micro channel without step at various Knudsen number and Pi/Po=2

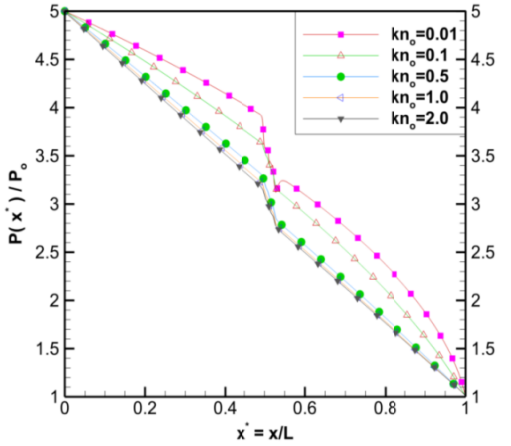

Fig. 32. Centerline pressure profile at different outlet Knudsen numbers and Pi/Po=5, Pressure Loss, 3 steps

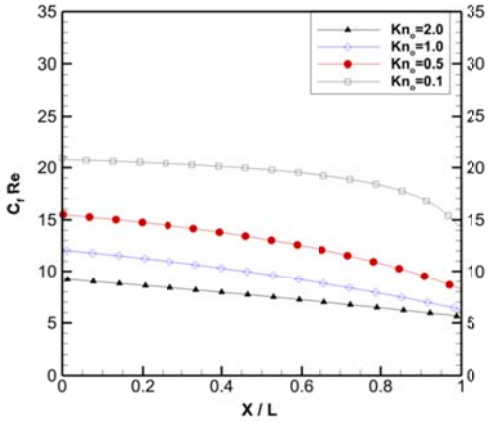

Fig. 35. Variation of friction coefficient throughout micro channel without step at various Knudsen number and Pi/Po=5

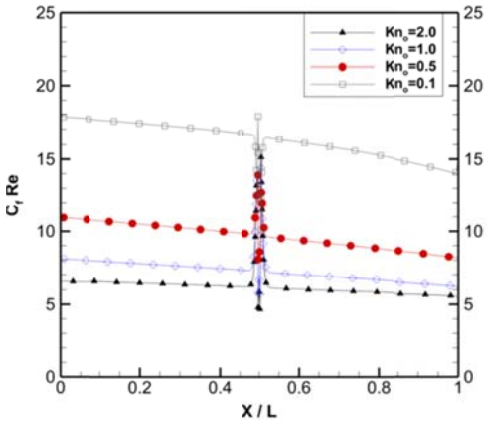

Fig. 36. Variation of friction coefficient throughout micro channel with three steps at various Knudsen number and Pi/Po=2

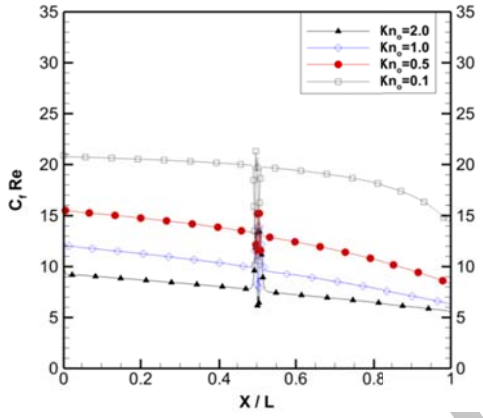

Fig. 37. Variation of friction coefficient throughout micro channel with three steps at various Knudsen number and Pi/Po=5

Friction coefficient is a basic concept which shows wall shear stress in the flow field in general and estimation of its value helps us to calculate the required power to creation the fluid flow in the system. Variation of friction coefficient in the micro-channel is shown in figures (33-37) which include the results for different Knudsen numbers, different pressure ratio and with steps in the micro-channel and without it. The steps have inverse effect on friction coefficient and cause its increasing. The variation of friction coefficient has presented in figure 33 versus Knudsen number and is compared with available data [38] and shows, the friction coefficient decreases with increasing the Knudsen number considerably. Our suggested correlation for friction coefficient as function of Knudsen number is as blow;

$$C_f Re = 3.113 + \frac{2.915}{1 + 2\,Kn} + 0.641 \exp\left(\frac{3.203}{1 + 2\,Kn}\right) \quad (41)$$

4. Conclusion

In this research, the fluid flow of gases has been analyzed in the stepped micro-channel for wide range of Knudsen number with using the Lattice Boltzmann method. It includes the slip and transition regimes of flow. These results have been shown;

1- Friction coefficient decreases with increasing Knudsen number, so the friction coefficient takes lower value in slip and transition regimes in compared with no-slip regime of flow.

2- Considering the steps in the micro-channel has inverse effect on friction coefficient and causes, the friction coefficient increasing at steps location, so the mean value of friction coefficient will higher in the stepped micro-channel in compared with simple micro-channel.

3- The centerline velocity of micro-channel has higher values in low Knudsen numbers due to compressibility effect of fluid flow.

4- With increasing the Knudsen number, the slip velocity at the wall increases and this results higher value of mean velocity and velocity profile flats in the cross section of micro-channel.

5- A new correlation for calculation of friction coefficient in the micro-channel at slip and transition regimes has been suggested.

References

[1] H. Xue, S. Chen, DSMC Simulation of Microscale Backward-Facing Step Flow, Microscale Thermophysical Engineering 7 (2003) 69-86

[2] S. Ansumali, I. V. Karlin, Kinetic boundary conditions in the lattice Boltzmann method, Physical Review E 66 (2002) 026311.

[3] G. Karniadakis, A. Beskok, N. Aluru, Microflows and Nanoflows Fundamentals and Simulation, Springer, USA, 2005.

[4] R.W. Barber, D.R. Emerson, Challenges in Modeling Gas-Phase Flow in Microchannels: From Slip to Transition, Heat Transfer Engineering 27 (2006) 3-12.

[5] H. Lai, C. Ma, Lattice Boltzmann method for the generalized Kuramoto–Sivashinsky equation, Physica A, Statistical Mechanics and its Applications 388 (2009) 1405-1412.

[6] M. Sbragaglia, S. Succi, Analytical calculation of slip flow in lattice Boltzmann models with kinetic boundary conditions, Physics of Fluids (1994-present) 17 (2005).

[7] E.B. Arkilic, M.A. Schmidt, K.S. Breuer, Gaseous slip flow in long microchannels, Microelectromechanical Systems 6 (1997) 167-178.

[8] K. Pong, C. Ho, J. Liu, Y. Tai, Non-linear pressure distribution in uniform microchannels., in: Application of Microfabrication to Fluid Mechanics, ASME Winter Annual Meeting (1994) 51-56.

[9] G.E.K. Ali Beskok, A Model For Flows In Channels, Pipes, And Ducts At Micro And Nano Scales, Microscale Thermophysical Engineering 3 (1999) 43-77.

[10] J. Suehiro, G. Zhou, H. Imakiire, W. Ding, M. Hara, Controlled fabrication of carbon nanotube NO_2 gas sensor using dielectrophoretic impedance measurement, Sensors and Actuators B 108 (2005) 398-403.

[11] A. Agrawal, L. Djenidi, R.A. Antonia, Simulation of gas flow in microchannels with a sudden expansion or contraction, Journal of Fluid Mechanics (2005) 135-144.

[12] Z. Guo, T.S. Zhao, Y. Shi, Physical symmetry, spatial accuracy, and relaxation time of the lattice Boltzmann equation for microgas flows, Journal of Applied Physics 99 (2006).

[13] Z. Guo, B. Shi, T.S. Zhao, C. Zheng, Discrete effects on boundary conditions for the lattice Boltzmann equation in simulating microscale gas flows, Physical Review E 76 (2007) 056704.

[14] Z. Guo, C. Zheng, Analysis of lattice Boltzmann equation for microscale gas flows: Relaxation times, boundary conditions and the Knudsen layer, International Journal of Computational Fluid Dynamics 22 (2008) 465-473.

[15] Z. Guo, C. Zheng, B. Shi, Lattice Boltzmann equation with multiple effective relaxation times for gaseous microscale flow, Physical Review E 77 (2008) 036707.

[16] T. Lee, C.-L. Lin, Rarefaction and compressibility effects of the lattice-Boltzmann-equation method in a gas microchannel, Physical Review E 71 (2005) 046706.

[17] F. Verhaeghe, L.-S. Luo, B. Blanpain, Lattice Boltzmann modeling of microchannel flow in slip flow regime, Journal of Computational Physics 228 (2009) 147-157.

[18] X. Shan, X.-F. Yuan, H. Chen, Kinetic theory representation of hydrodynamics: a way beyond the Navier–Stokes equation, Journal of Fluid Mechanics (2006) 413-441.

[19] S. Ansumali, I.V. Karlin, S. Arcidiacono, A. Abbas, N.I. Prasianakis, Hydrodynamics beyond Navier-Stokes: Exact Solution to the Lattice Boltzmann Hierarchy, Physical Review Letters 98 (2007) 124502.

[20] Y.-H. Zhang, X.-J. Gu, R.W. Barber, D.R. Emerson, Capturing Knudsen layer phenomena using a lattice Boltzmann model, Physical Review E 74 (2006) 046704.

[21] G.H. Tang, Y.H. Zhang, X.J. Gu, D.R. Emerson, Lattice Boltzmann modelling Knudsen layer effect in non-equilibrium flows, EPL (Europhysics Letters) 83 (2008) 40008.

[22] A. Homayoon, A.H.M. Isfahani, E. Shirani, M. Ashrafizadeh, A novel modified lattice Boltzmann method for simulation of gas flows in wide range of Knudsen number, International Communications in Heat and Mass Transfer 38 (2011) 827-832.

[23] H. Shokouhmand, A.H. Meghdadi Isfahani, An improved thermal lattice Boltzmann model for rarefied gas flows in wide range of Knudsen number, International Communications in Heat and Mass Transfer 38 (2011) 1463-1469.

[24] S.S. Chikatamarla, I.V. Karlin, Entropy and Galilean Invariance of Lattice Boltzmann Theories, Physical Review Letters 97 (2006) 190601.

[25] T. Ohwada, Y. Sone, K. Aoki, Numerical analysis of the shear and thermal creep flows of a rarefied gas over a plane wall on the basis of the linearized Boltzmann equation for hard-sphere molecules, Physics of Fluids A: Fluid Dynamics 1 (1989) 1588-1599.

[26] P. Lallemand, L.-S. Luo, Theory of the lattice Boltzmann method: Dispersion, dissipation, isotropy, Galilean invariance, and stability, Physical Review E 61 (2000) 6546-6562.

[27] C.Y. Lim, C. Shu, X.D. Niu, Y.T. Chew, Application of lattice Boltzmann method to

simulate microchannel flows, Physics of Fluids (1994-present) 14 (2002) 2299-2308.
[28] V. Michalis, A. Kalarakis, E. Skouras, V. Burganos, Rarefaction effects on gas viscosity in the Knudsen transition regime, Microfluid Nanofluid 9 (2010) 847-853.
[29] S.H. Kim, H. Pitsch, I.D. Boyd, Slip velocity and Knudsen layer in the lattice Boltzmann method for microscale flows, Physical Review E 77 (2008) 026704.
[30] S.H. Kim, H. Pitsch, I.D. Boyd, Accuracy of higher-order lattice Boltzmann methods for microscale flows with finite Knudsen numbers, Journal of Computational Physics 227 (2008) 8655-8671.
[31] Y. Zhang, R. Qin, D.R. Emerson, Lattice Boltzmann simulation of rarefied gas flows in microchannels, Physical Review E 71 (2005) 047702.
[32] Y.-H. Zhang, X.J. Gu, R.W. Barber, D.R. Emerson, Modelling thermal flow in the transition regime using a lattice Boltzmann approach, EPL (Europhysics Letters) 77 (2007) 30003.
[33] S. Succi, Mesoscopic Modeling of Slip Motion at Fluid-Solid Interfaces with Heterogeneous Catalysis, Physical Review Letters 89 (2002) 064502.
[34] M.N. Oliveira, L. Rodd, G. McKinley, M. Alves, Simulations of extensional flow in microrheometric devices, Microfluid Nanofluid 5 (2008) 809-826.
[35] T.-M. Liou, C.-T. Lin, Study on microchannel flows with a sudden contraction–expansion at a wide range of Knudsen number using lattice Boltzmann method, Microfluid Nanofluid, 16 (2014) 315-327.
[36] L. Talon, D. Bauer, N. Gland, S. Youssef, H. Auradou, I. Ginzburg, Assessment of the two relaxation time Lattice-Boltzmann scheme to simulate Stokes flow in porous media, Water Resources Research 48 (2012) W04526.
[37] S. Kandlikar, S. Garimella, D. Li, S. Colin, M. King, Heat Transfer and Fluid Flow in Minichannels and Microchannels, Elsevier Amsterdam, Netherlands, San Diego, CA, Oxford, UK, 2005.
[38] H.P. Kavehpour, M. Faghri, Y. Asako, Effects of compressibility and rarefaction on gaseous flows in microchannels, numerical heat transfer, part a: applications 32 (1997) 677-696.